This is a peer-reviewed, accepted author manuscript of the following article: Aniagor, C. O., Elshkankery, M., Fletcher, A. J., Morsy, O. M., Abdel-Halim, E. S., & Hashem, A. (Accepted/In press). Equilibrium and kinetic modelling of aqueous cadmium ion and activated carbon adsorption system. *Water Conservation Science and Engineering*.

# Equilibrium and kinetic modelling of aqueous cadmium ion and activated carbon adsorption system

Chukwunonso O. Aniagor[a*], M. Elshkankery[b], A. J. Fletcher[c], Osama M. Morsy[b], E. S. Abdel-Halim[b], A. Hashem[b**]

[a]*Department of Chemical Engineering, Nnamdi Azikiwe University, P.M.B. 5025, Awka, Nigeria*
[b]*Textile Research Division, National Research Centre, Dokki, Cairo, Egypt.*
[c]*Department of Chemical and Process Engineering, University of Strathclyde, 75 Montrose Street, Glasgow, G1 1XJ, UK.*

*Corresponding authors' e-mail: co.aniagor@unizik.edu.ng
**Corresponding authors' e-mail: alihashem2000@yahoo.com

**ORCID**

Chukwunonso .O. Aniagor: http://orcid.org/0000-0001-6488-3998
A. Hashem: https://orcid.org/0000-0001-7981-4872

## Abstract

Despite their extensive and decade long application in wastewater treatment, activated carbon remains one of the most viable adsorbents, with substantive practical application, due to their high pollutant binding capacity. In this study, commercially available activated charcoal was applied in the uptake of aqueous cadmium [Cd(II)] ion. The effect of some process variables on the Cd (II) uptake was investigated via batch mode. Furthermore, the adsorbents' surface charge ($pH_{PZC}$), surface morphology (using SEM) and available surface functional groups (using FTIR) were explained. The pH dependence of the present adsorption system was revealed, with the optimum pH was recorded at pH 5.0. Similarly, the Cd (II) uptake (mg/g) decreased with increasing adsorbent dosage due to possible active sites clogging, overcrowding and interference Furthermore, the isothermal and kinetics analyses of the experimental data, that were aptly validated using the hybrid error model, respectively depicted the Langmuir isotherm and pseudo-second-order kinetic model as the best fit. A Langmuir adsorption capacity of 682.5 mg $g^{-1}$ was also recorded in the study. Consequently, the present adsorption system was characterized by an equilibrium timeframe of industrial practicability, hence the adsorbent was successfully applied for the aqueous Cd (II) uptake.

***Keywords***: Activated carbon, cadmium, isotherm, kinetics, adsorption

## 1. Introduction

Heavy metals are one of the major polluting constituents of industrial effluents, which may subsequently find their way into the food chain, thereby causing serious health problems [1]. The heavy metal toxicity is mainly due to their non-biodegradability when compared to most organic wastes [2]. The Cd (II), our adsorbate of choice, owe its presence in the aquatic environment to several industrial activities, such as oil refining, mining, alloys manufacturing, metal electro-plating, etc [3]. Cadmium ions' high toxicity is linked to their bioaccumulation potentials, even at very low concentration levels [4]. Disease-related to Cd (II) bioaccumulation in humans include kidney stone/infection, hypertension, proteinuria, etc [5]. Also, the ability of cadmium ion to displace the zinc ion content of certain enzymes and disrupt normal enzymatic functionality has been reported [6]. The aforementioned consequences of cadmium ion pollution warrant a comprehensive approach to their dissipation from the aqueous environment [7].

Adsorption is regarded as one of the most economical and effective techniques for the sequestration of aqueous organic and inorganic pollutants from a variety of sources [8]. In contrast with other conventional treatment techniques (such as reverse osmosis, ion exchange, electro-deposition and precipitation), adsorption offer the advantages of cost-effectiveness, high operational flexibility and high efficiency. Cadmium ion has been previously sequestered using different material like nano zero-valent iron [9], ground wheat stems [10], Surfactant-modified chitosan beads [11], hydrochar [12], copper-based metal-organic framework [13], modified pinewood sawdust [14], aminated acrylic fibre [15], etc.

Meanwhile, some of these adsorbents are prohibitively expensive in the event of extensive application in the field of wastewater treatment (especially in developing countries), due to start-up and maintenance costs [16]. To this end, studies have focused on the development of adsorbents from industrial by-products and agricultural residues, such that possess high organic and metal ion sorption capacities [17, 18]. This approach does not only offer economic benefits, (in term of low water treatment operational cost) but is also considered as readily available renewable adsorbent resources [16, 19]. Most of the adsorbents are manufactured locally using charcoal burners, thereby reducing costs [20]. Consequently, activated carbon (AC) has sustained proven applications in toxic material uptake, even at low aqueous concentration [21]. To date, AC remains an excellent adsorbent for wastewater reclamation due to its high sorption capacity

which is related to its large surface area, pore size distribution and mechanical stability [22]. Their hydrophobic and hydrophilic graphene layers and functional groups, respectively, also aid their application as adsorbents in the uptake of ionic species [23] and catalyst support applications [24].

**Osasona, *et al* [25]** studied the adsorption of Cd (II) onto spent barley husks AC. The study reported the dependence of the heavy metal uptake capacity on the process variable, hence, a maximum adsorption capacity of 6.64 mg $g^{-1}$ was recorded at 5 min and pH 6.0. Nejadshafiee*, et al* [26] studied the effectiveness of sultone functionalization and magnetization on the Cd (II) adsorption performance of pistachio shell AC. The adsorptive study was however reported as effective, with a maximum adsorption capacity of 119.04 mg $g^{-1}$. Olive branch activated carbon was also applied in the adsorption of aqueous Cd (II) [27]**.** The study reported the prevalence of endothermic process at pH 5.0, with a maximum adsorption capacity of 38.17 mg $g^{-1}$. At varying reaction conditions (adsorption concentration of 250 mg/L and contact time of 180 and pH 6.0), Manjuladevi*, et al* [28] recorded a Cd (II) uptake efficiency of 97.96 % using *Cucumis melo* peel AC. Furthermore, a different blend of AC composites including activated carbon/zirconium oxide composite [29]**,** polyethyleneimine modified AC [30] and magnetic AC [31] have been successfully applied in the uptake of aqueous Cd (II).

The literature survey has outlined arrays of functionalized activated carbon adsorbent (based on different modification techniques) applied for the adsorptive uptake of aqueous cadmium ion. However, the application of most of these functionalized/hybrid ACs in water treatment was mostly good at laboratory scale and for mere academic exercise. This is because most of the functionalized AC adsorbents lack extensive real-life and industrial applications. According to Ioannidou*, et al* [32], a well prepared AC in its purest form possesses all the attributes and characteristics necessary for pollutant binding. To this end, the present study aims to examine the adsorption capacity of commercially available activated charcoal for cadmium ions uptake. The AC was instrumentally characterized and the effect of specified process variables (initial solution pH, contact time and adsorbent dosage) was also elucidated. Similarly, the generated experimental data were subjected to non-linearly regressed equilibrium and kinetics modelling and further validated using an error model.

## 2. Materials and methods

### 2.1. Materials

Activated charcoal was kindly supplied by El-Gomhoreya Chemicals Company, Cairo, Egypt. All the laboratory-grade chemicals used in the study, sodium hydroxide (NaOH), nitric acid ($HNO_3$), cadmium acetate and ethylenediaminetetraacetic acid (EDTA) were supplied by Merck (Germany).

### 2.2. Batch adsorption studies

The AC sample (~0.05 g) was accurately measured into 100 mL of Cd (II) solutions (in the concentrations range of 100-1150 mg $L^{-1}$) contained in series of 125 mL Erlenmeyer flasks. The adsorbate solution pH was adjusted to the desired value via dropwise addition of 0.1 M NaOH or 0.1 M $HNO_3$, as required. The content of the respective flasks was continuously stirred at 150 rpm (using a mechanical magnetic stirrer) for a specified duration (between 5 and 300 min), while the solution temperature was maintained isothermally in a water bath. Afterwards, the spent adsorbent was obtained as residue from the solution. Meanwhile, the amount of cadmium ion adsorbed at a given time was determined by titrating the filtrate against a standard EDTA solution. The amount of Cd (II) ions adsorbed at equilibrium, $q_e$ (mg $g^{-1}$) and the percentage Cd (II) removed is calculated using Eqs. (1 – 2), respectively.

$$q_e = \frac{(C_o - C_e)\cdot V}{W} \quad (1)$$

$$\% \text{ Removal} = \frac{C_o - C_e}{C_o} \times 100 \quad (2)$$

Where $C_e$ and $C_o$ (mg $L^{-1}$) are initial and equilibrium metal concentrations, W (g) is the mass of adsorbent used and V (L) is the Cd (II) ion solution volume.

### 2.3. Adsorbent analysis

The adsorbent samples were prepared for SEM imaging by coating them with a thin layer of gold metal using a diode sputter unit and then imaged using a Scanning Electron Microscope (Model JEOL-JSM-5600) with an accelerating voltage of 25.0 kV.

The energy dispersive X-ray pattern (EDX) of the activated charcoal adsorbent post-adsorption with Cd (II) ions was measured using a dispersive X-ray fluorescence (EDX) spectrometer

(Oxford Instruments) attached with the aforementioned Scanning Electron Microscope to confirm Cd(II) ion adsorption through the absence or presence of the characteristic band of cadmium metal.

The surface charge of the adsorbent was determined by evaluating the pH at the point of zero charges ($pH_{PZC}$). The initial pH value ($pH_{initial}$) of several flasks containing 100 mL of 0.01 N NaCl solution was adjusted using either 0.01 N NaOH solution or 0.01 N HCl solution to obtain a suite of solutions in the range pH 2.0 – 11.0. To each NaCl solution of a certain $pH_{initial}$, precisely 0.1 g of adsorbent was added. The pH of each NaCl solution was measured again, after 24 h of contact time with the adsorbent, this second value was denoted $pH_{final}$, and plotted against $pH_{initial}$. The $pH_{PZC}$ for the adsorbent was defined as the point at which $pH_{initial}$ was equal to the $pH_{final}$.

## 2.4. Adsorption isotherm modelling

The adsorption isotherm is a mathematical model that relates the equilibrium amount of the adsorbate immobilized onto the adsorbent surface ($q_e$) to those remaining in the bulk of the solution ($C_e$). Several isotherm models have been documented for describing the experimental data obtained for a range of adsorption processes. In this study, three 2-parameter models, namely, the Langmuir, Temkin and Freundlich models, were applied for fitting the experimental equilibrium data. The theory associated with the respective isotherm models is discussed in the following subsection.

### 2.4.1. Langmuir Isotherm

The Langmuir model [33] postulates the occurrence of monolayer adsorption onto a fixed number of localised sites on an adsorbent surface. The model further assumes that a given adsorbent surface is composed of an array of surface sites that is homogeneously equivalent in their enthalpies but with no subsequent movement of adsorbed molecules in the surface plane, as well as no interactions between neighbouring adsorbate molecules. The non-linear expression of the Langmuir isotherm is given by **Eq. (3).**

$$q_e = \frac{q_m k_L C_e}{1 + k_L C_e} \tag{3}$$

where $K_L$ (L $g^{-1}$) is the Langmuir isotherm constants, $q_m$ is the maximum adsorption capacity (mg $g^{-1}$), $C_e$ is the adsorbate concentration at equilibrium (mg $L^{-1}$), and $q_e$ is the amount of Cd

(II) ions adsorbed per unit mass of adsorbent (mg $g^{-1}$). $K_L$ can be used to determine the dimensionless separation factor, $R_L$, which indicates the favourability of the adsorption process, and is given by **Eq. (4)** [34, 35].

$$R_L = \frac{1}{1+(K_L \cdot C_o)} \quad (4)$$

where $C_o$ is the initial adsorbate solution concentration and the constant. Adsorption is considered unfavourable when $R_L > 1$, linear if $R_L = 1$, favourable for $0 < R_L < 1$, and irreversible when $R_L = 0$.

2.4.2. Freundlich Isotherm

The Freundlich isotherm model is based on the formation of limitless multilayer of adsorbed species, with infinite surface coverage predicted on a heterogeneous surface. The enthalpies of the adsorbent surface sites follow a logarithmic distribution, where the higher energy sites, i.e. those with a higher affinity for the adsorbate, are occupied first, followed by the lower energy sites. The sorption process is summed across sites, and the logarithmic expression of the Freundlich model is given by **Eq. (5)** [36, 37].

$$q_e = K_F(C_e)^{\frac{1}{n_F}} \quad (5)$$

where $C_e$ and $q_e$ are as defined above; $K_F$ and n are the two Freundlich constants, related to the capacity of adsorption and favourability of adsorption, respectively. In particular, the value of n indicates the favourability of the adsorption process. When '*n-value'* falls between 2 and 10, favourable adsorption is implied, while '*n-value'* less than unity indicates poor sorption characteristics [37].

2.4.3. Temkin Isotherm

Similar to the Freundlich isotherm model, the Temkin isotherm model [38] postulates the heterogeneity of an adsorbent surface, whose adsorption energy distribution is linear. The non-linear form of the Temkin isotherm model given by **Eq. (6).**

$$q_e = \frac{RT}{b_T}\ln(K_T C_e) \quad (6)$$

where $C_e$ and $q_e$ are as defined above; T (K) is the absolute temperature, R is the universal gas constant (8.314 J $mol^{-1}$ $K^{-1}$), while $A_T$ (L $g^{-1}$) and $b_T$ (J $mol^{-1}$) are the two Temkin isotherm constants, the latter being related to the heat of adsorption,

## 2.5. Adsorption kinetic modelling

Kinetic models were applied to predict the kinetics of Cd (II) ion adsorption onto the AC. This study is necessary for evaluating the effectiveness of an adsorption process and identifying the type/nature of the adsorption mechanisms [39]. In the current study, three kinetic models were applied namely, pseudo-first-order (PFO), pseudo-second-order (PSO) and intra-particle diffusion models.

### 2.5.1. Pseudo-first-order model

A pseudo-first-order kinetic model is applied to a system where the adsorption process is usually considered as diffusion-controlled and physisorption. The non-linear mathematical representation of a pseudo-first-order model [40] is given by **Eq. (7).**

$$q_t = q_e[1 - \exp(-k_1 t)] \quad (7)$$

where $q_t$ (mg $g^{-1}$) is the amount of Cd (II) ions adsorbed at a given contact time t (min), $q_e$ (mg $g^{-1}$) is the amount of Cd (II) ions adsorbed at equilibrium, and $k_1$ ($min^{-1}$) is the rate constant.

### 2.5.2. Pseudo-second-order (PSO) model

This model assumes that the adsorption rate is controlled by the sharing of electrons between the adsorbate and the adsorbent i.e. the adsorption process is considered as a chemical process. The mathematical expression of a pseudo-second-order kinetic model [41] is given by Eq. (8).

$$q_t = \frac{k_2 * q_e^2 * t}{(1 + k_2 * t)} \quad (8)$$

where $q_t$, $q_e$ and t are already defined above, and $k_2$ (g $mg^{-1}$ $min^{-1}$) is the PSO rate constant.

### 2.5.3. Intra-particle diffusion model

According to Aniagor*, et al* [39], the shape of a plot of $q_t$ vs. $t^{1/2}$ is often a series of separate sections that represent different control mechanisms during the adsorption process. The kinetics of adsorption, when controlled by an intra-particle diffusion kinetic model, can be expressed as **Eq. (9) [42].**

$$q_t = k_{id} t^{0.5} \quad (9)$$

where $q_t$, $q_e$ and t are already defined above; $k_{id}$ (mg $g^{-1}$ $min^{-1}$) is the intra-particle diffusion rate constant and C is a constant that represents the boundary layer thickness.

2.6. Error function

For non-linear regression, coefficient of determination ($R^2$) values has been reported as insufficient for evaluating its goodness of fits; thus the application of error models [43, 44]. Similarly, El-Khaiary*, et al* [45] observed that the data prediction performance of a given nonlinear model is mostly a function of the number of their inherent parameters [45, 46]. Therefore, the number of fitting parameters of the respective isotherm or kinetic model is considered when evaluating the error variance in their experimental data prediction. In this study, the Hybrid fractional error model is applied because it considered the number of fitting parameters. The mathematical expression of the hybrid fractional (HYBRID) error function is shown in **Eq. (10).**

$$HYBRID = \frac{100}{n-p}\sum\left[\frac{(q_{e,exp}-q_{e,Calc})^2}{q_{e,exp}}\right] \quad (10)$$

## 3. Results and discussion

3.1. Analyses of the AC surface morphology

**Figure 1** presented the scanning electron micrograph of AC before adsorption and after Cd (II) adsorption. The pre-adsorption image (**Figure 1a**) is characterized by surface heterogeneity/roughness and the semblance of irregular layers, while **Figure 1b** presented a smoother morphology. The more pronounced surface roughness observed in **Figure 1a** provided unmistakable proof for the existence of a large number of cavities and pores. Hence, the chemical activation of the charcoal improved their surface properties and porosity, as well as introduced good surface morphology, capable of metal ion binding. The pores initially present in **Figure 1a** provided active sites for the Cd (II) uptake and also enhanced the diffusion of Cd (II) ion through the AC structure. This occurrence subsequently afforded an improved surface area for adsorbate-adsorbent complexation. The said complexation phenomenon further explains the smooth surface morphology observed in **Figure 1b**. The presence of an irregular rough surface that is synonymous with surface porosity also characterized the activated carbon synthesized by Xie*, et al* [30] for Cd (II) uptake. The study believed that the surface roughness afforded more adsorption sites for heavy metal adsorption. Similarly, in line with our findings, Sharma*, et al* [29] and Zhang*, et al* [31] reported the smoothening and homogenization of the activated carbon surface due to the loss of their porous structure sequel to Cd (II) adsorption.

Additional confirmation for the adsorption of the Cd (II) ion onto the AC surface is provided with the Energy Dispersion X-ray (EDX) spectrum shown in **Figure 1c.** Judging from the Figure, the appearance of clear and sharp cadmium characteristics signals confirms the presence of the Cd (II) ion on the spent AC adsorbent surface.

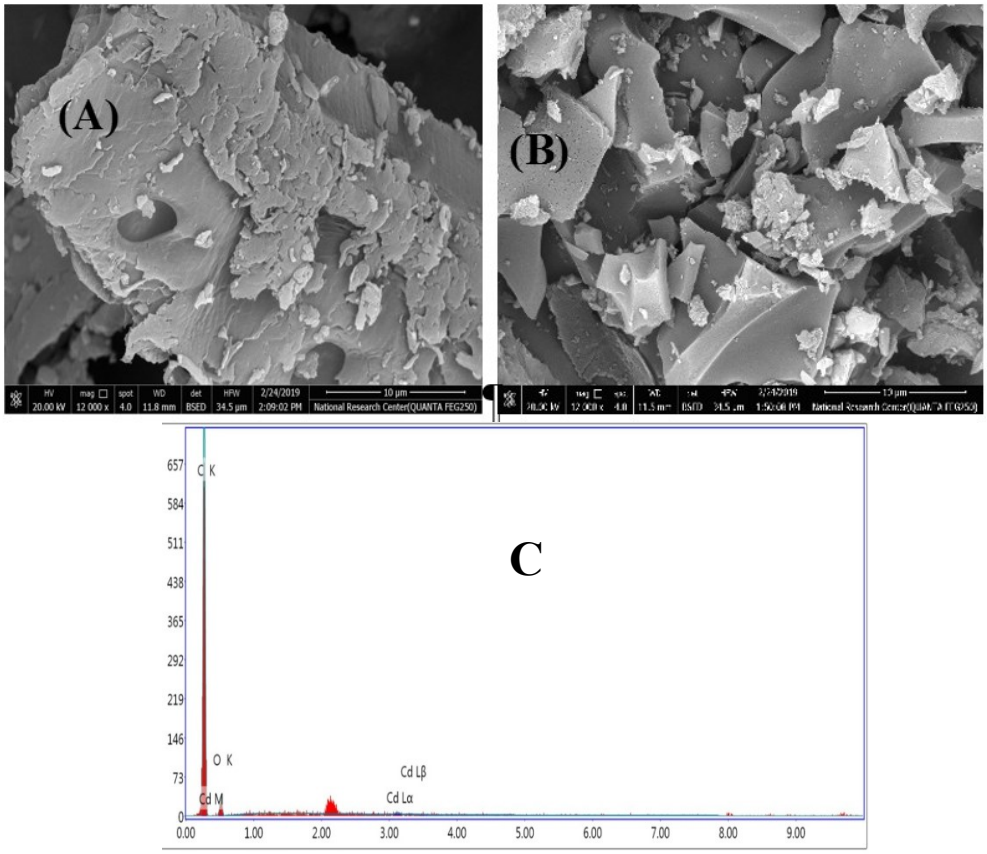


**Figure 1:** SEM images of unused AC (A), spent AC (B) and EDX result (C)

3.2. Analyses of the AC surface chemical

**Figure 2** shows the FTIR spectra for the unused and spent AC adsorbent. The spectra of the unused AC are characterized by some notable peaks around 2900 $cm^{-1}$ (–CH stretch), 2100 $cm^{-1}$ (C ≡ N stretch) and 1450 $cm^{-1}$ (-$CH_2$ bend). A broad peak that represented the –OH groups due to the possible oxidative treatment of the AC precursor was identified between 3000 - 3600 $cm^{-1}$. The peak at 1800 $cm^{-1}$ and around 900 $cm^{-1}$ is assigned to the carbonyl group and C-O-O-stretch, respectively **[47].** Meanwhile, the comprehensive FTIR raw data illustrated that asides from the aforementioned groups, the oxidative treatment also introduced numerous other

oxygen-based functional groups, whose assemblage is not sufficient to institute prominent peaks. Other authors who applied varying form of activated carbon to adsorb Cd (II) also identified the presence of some oxygen-containing functional groups, such as carboxyl, hydroxyl, and ether groups, on the adsorbent surface [29, 30]. Their findings point to the usefulness of these oxygen-based functional groups in metal ion sequestering. Furthermore, the peak existing around 1010 $cm^{-1}$ is assigned to the –C=N groups, occurring due to a probable cyclization of the $C \equiv N$ groups on the AC precursor **[48].** The FTIR of the spent AC quite similar to those of the raw AC except for some slight variations in the % transmittance (see Figure 2)

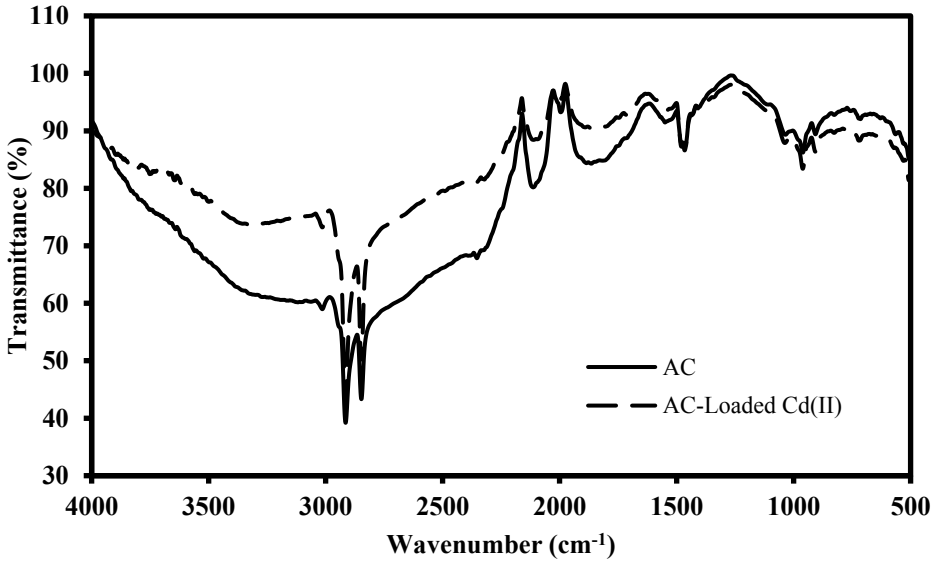


**Figure 2:** The FTIR spectra for the activated carbon

3.2. Studies on the effect of process variables

3.2.1. Point of zero charge ($pH_{PZC}$) and the effect of pH

The value of $pH_{PZC}$ provides insight into the nature of electrostatic interaction arising between the adsorbent surface and adsorbate molecules [49]. According to Nwosu*, et al* [50], $pH_{PZC}$ is the pH value at which a given adsorbents' surface possesses a net neutral charge. Studies [51, 52] have also shown that at adsorbate solution pH values higher than the $pH_{PZC}$, the adsorbent surface will be predominately negative and vice versa [53]. From **Figure 3a,** the $pH_{PZC}$ of AC was recorded at pH 4.1, an indication of the relative surface acidity of the AC. Based on this finding, the operational solution pH during cadmium ion adsorption is expected to be higher than pH 4.1 to ensure efficient cation uptake via electrostatic interaction.

**Figure 3b** shows the influence of initial adsorbate solution pH on Cd (II) ion adsorption in the range pH 2.0 – 6.0 at a constant initial concentration of 200 mg $L^{-1}$. The plot illustrated an increase in the amount of adsorbed Cd (II) ion ($q_e$) from 2 mg $g^{-1}$ to 126 mg $g^{-1}$, as solution pH increases beyond pH 2.0 and further attainment of a plateau at pH 5.0. Hence the study on the solution pH variation for the study was discontinued at pH > pH 6.0. The marked increase in the adsorbed adsorbate amount with pH increase (from pH 2.0 – pH 5.0) is attributed to deprotonation of the charcoal surface at pH > $pH_{PZC}$ (i.e. more basic pH values). Thus, the deprotonated AC surface consequently underwent an electrostatic interaction with the cadmium cations to entrench optimal pollutant chelation. Notably, the amount of Cd (II) ions adsorbed at pH 2.0 is almost zero. This occurrence is due to the high AC surface protonation at such acidic medium which heightened the incidence of adsorbate-adsorbent electrostatic repulsion, thus favouring the backward reaction (cadmium ion desorption) [54]. Meanwhile, at a higher pH range (pH > 5.0) the Cd (II) ion got precipitated and exists mostly as an insoluble $Cd(OH)_2$. Therefore, the optimum solution pH was recorded at pH 5.0 (**Figure 3b**). At this pH value, the AC surface charge was predominantly negative and thus implies an efficient adsorbent-adsorbate electrostatic attraction [55]. The optimal pH value obtained in this study was collaborated by other authors who reported the precipitation of cadmium ion as insoluble hydroxide beyond pH 5.0 [10, 23].

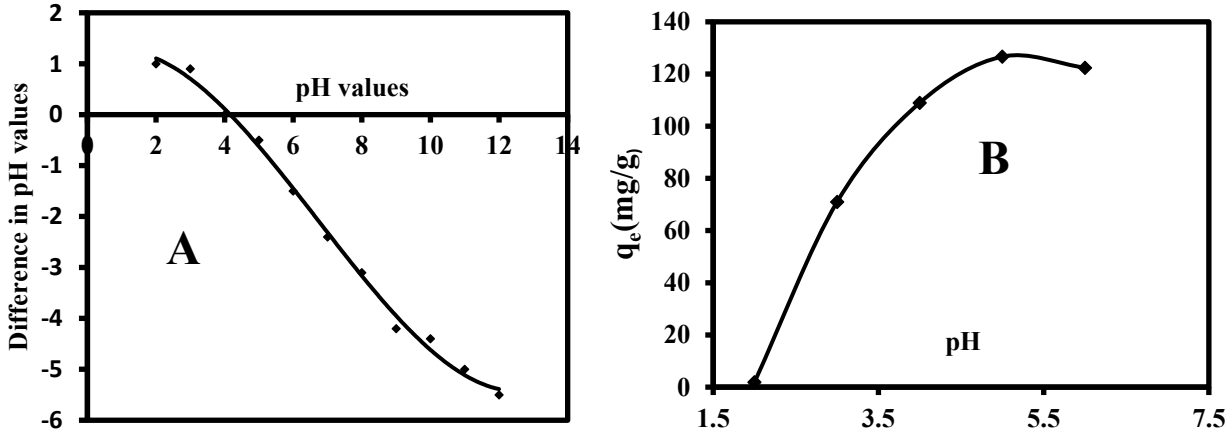


**Figure 3:** (a) potentiometric titration plot (b) Effect of solution pH on the adsorption capacity

3.2.2. Effect of adsorbent dose

Metal ion uptake is greatly affected by the adsorbent dose, and their concentration effect on the AC adsorption capacity was studied in the range of 0.3 to 10 g $L^{-1}$ at constant pH (pH 5.0) and

adsorbate concentration (200 mg $L^{-1}$). **Figure 4** depicted that the amount of Cd (II) ions adsorbed per unit mass of adsorbent (mg $g^{-1}$), consistently decreases from 129.44 mg $g^{-1}$ (at 0.3 g/L) to 19 mg $g^{-1}$ with increasing adsorbent dose up to 6.0 g $L^{-1}$, after which a plateau was achieved (beyond 6.0 g/L dosage). Thus, the highest sorption capacity of 129.44 mg $g^{-1}$ was recorded at the least sorbent concentration of 0.3 g/L. This inverse relationship between the adsorption capacity and adsorbent dosage is explained by the fact that high adsorbate-adsorbent site affinity predominated at the initial low adsorbent dosage (0.2 g/L) [56]. Meanwhile, with the increasing adsorbent concentration (from 0.3 to 10.0 g/L) the sorption capacity consistently diminished (despite the supposed increase in available sorption sites), due to possible active sites clogging, overcrowding and interference [52]. Using different modified activated carbon, Alhan*, et al* [57] and Nejadshafiee*, et al* [26] also reported a similar variation between the heavy metal uptake capacity and the adsorbent dosage.

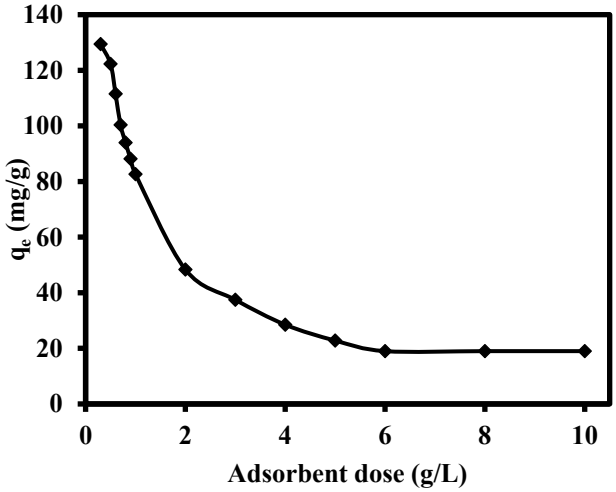


**Figure 4:** Effect of adsorbent dose on adsorption capacity

3.3. Isothermal adsorption analyses

Three **(3)** nonlinear isotherm model, namely Langmuir, Freundlich and Temkin models were applied for modelling the present adsorption system. The isotherm parameters generated from the models, together with the goodness-of-fit values ($R^2$ and ARE) are presented in **Table 1.** Generally, the isotherm model parameters provide reasonable information on the nature of the adsorption system. For instance, when the Langmuir separation factor, ($R_L$) is either greater than or equal to unity, the adsorption process is considered to be linear and unfavourable,

respectively. Similarly, when the $R_L$ value is greater than zero but less than unity, a favourable adsorption system is implied, while, irreversible adsorption is signified by $R_L = 0$. Furthermore, the Freundlich model indicates a linear, chemical and physical nature of an adsorption system when $n_F = 1$, $n_F < 1$ and $n_F > 1$, respectively. The Temkins' adsorption energy variation constant, $b_T$ indicates an exothermic (when $b_T$-value is positive) and endothermic (when $b_T$-value is negative) process.

**Table 1** depicted the Langmuir isotherm as the model of best fit since it showed the lowest Hybrid error value (0.490), as well as a reasonably high $R^2$ value (0.995) when compared to that of Freundlich models (Hybrid = 0.542, $R^2$ = 0.996) and Temkin (Hybrid = 0.974, $R^2$ = 0.963). This result then follows the fact that the cadmium ion adsorption predominantly occurred on a homogenous monolayer surface [33], with minimal interaction with adjacent adsorbate molecules. The Langmuir model fit also gave an $R_L$ value of 0.0012 ($0 < R_L < 1$), indicating favourable adsorption of Cd (II) onto the AC surface. It should be noted that the Freundlich and Temkin model also provided a reasonably good fit to the experimental adsorption data, although, their fitting goodness is marginally inferior to the Langmuir model fit over the entire analytical range. Hence, asides Langmuir model, one can safely make additional inference on the implication of the Freundlich and Temkin model parameters to the current adsorption system. For instance, the Freundlich heterogeneity constant, $n_F$ was found to be 1.76 ($0 < n < 10$), again indicating the favourability of this process. However, the inverse value ($1/n_F$) of the heterogeneity constant is lower than unity and as such suggests a slight suppression in Cd (II) ion adsorption at lower equilibrium concentrations [56]. A positive value of $b_T$ constant depicted in **Table 1** indicates the exothermicity of the cadmium ion adsorption ono AC.

Consequently, the Langmuir adsorption capacity ($q_{max}$) value was determined as 682.5 mg $g^{-1}$ **(Table 1**), an indication of a strong adsorbate-adsorbent affinity when compared to other reported adsorbents (see **Table 2**). **Figure 5** was employed as further confirmation for the isotherm model adequacy at predicting the experimental data. The plot showed that the Langmuir data curves depicted a close relationship with the experimental data curve. This finding further confirms the goodness of the Langmuir model fit to the studied adsorption system.

**Table 1:** The isotherm model parameters and goodness of fit values

| Langmuir | Freundlich | Temkin |
|---|---|---|
| $q_{max}$ = 682.5 | $n_F$ = 1.76 | $A_T$ = 67.271 |
| $K_L$ = 0.879 | $K_F$ = 13.014 | $b_T$ = 60.02 |
| $R_L$ = 1.2E-03 | $R^2$ = 0.996 | $R^2$ = 0.963 |
| $R^2$ = 0.995 | HYBRID = 0.542 | HYBRID = 0.974 |
| HYBRID = 0.490 | | |

**Table 2:** Comparison of adsorption capacities of various sorbents for Cd (II) ions

| **Adsorbent** | **Adsorption capacity (mg/g)** | **Ref.** |
|---|---|---|
| AC from Spent Barley Husks | 6.64 | [25] |
| Olive branches AC | 38.17 | [27] |
| sultone-modified magnetic AC | 119.04 | [26] |
| AC/Zirconium oxide composite | 166.70 | [29] |
| Polyethyleneimine modified AC | 45.0 | [30] |
| Activated charcoal | 682.5 | Present study |

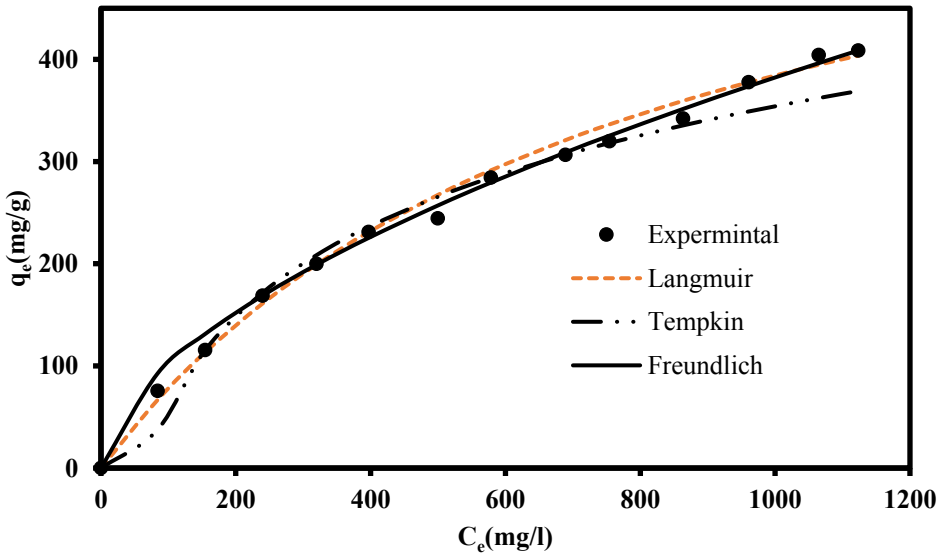


**Figure 5:** The Isotherm model plot

### 3.4. Adsorption kinetics

The plot of the effect of contact time and the kinetic models are presented in **Figure 6 (a-b). Figure 6a** showed that the adsorption uptake increases sharply with increasing contact time, reaching 111.0 mg $g^{-1}$ within 60 min. As the contact time further extended being 60 min, only a minor adsorption capacity increment occurs, and the process subsequently plateaued after 120 min. This means that complete equilibrium was achieved within the 60 min of adsorptive operation, which is relatively fast and shows the potential of this material in wastewater treatment.

The kinetic experimental data from the study was modelled with three (3) kinetic models namely, pseudo-first-order, pseudo-second-order and intraparticle particle diffusion model. The generated kinetic parameters are presented in **Table 3,** alongside the goodness of fit values. It is however evident that the Cd (II) adsorption onto AC follows a pseudo-second-order model due to its lowest hybrid error and highest $R^2$-value of 3.015 and 0.979, respectively. This development suggests a chemically controlled process, with minimal evidence of physical process. The inferior data fitting produced by the pseudo-first-order and intraparticle diffusion models were also noted, as they both depicted relatively high hybrid error values. Meanwhile, the intraparticle diffusion model parameter provides further insight into the prevalent adsorption mechanism. Table 3 depicts an intraparticle diffusion c-value of 63.30 and based on literature reports, such a high value ($c >>> 1$) is synonymous with the occurrence of substantive boundary layer effect within the system [52]. Thus, intraparticle diffusion cannot be regarded as a probable sorption mechanism in the study [58]. Conclusively, the trend of kinetic model goodness of fit is presented as follows: pseudo-second-order > pseudo-first-order > Intraparticle diffusion model. The above trend of result is confirmed from the experimental and predicted kinetic data shown in Figure 6b, where the pseudo-second-order curve line depicted the closest correlation with the experimental curve line.

**Table 3:** The kinetic model parameters and goodness of fit values

| Pseudo first order | Pseudo second order | Intraparticle diffusion |
|---|---|---|
| $q_e$ = 110.0 | $q_e$ = 122.0 | $k_{id}$ = 4.72 |
| $k_1$ = 0.089 | $k_2$ = 0.0014 | C = 63.30 |
| $R^2$ = 0.913 | $R^2$ = 0.979 | $R^2$ = 0.764 |
| HYBRID = 17.481 | HYBRID = 3.015 | HYBRID = 32.507 |

*$k_1$ ($min^{-1}$), $k_2$ (g $mg^{-1}$ $min^{-1}$), $q_e$ (mg $g^{-1}$) and $k_{id}$ (mg $g^{-1}$ $min^{-1}$)

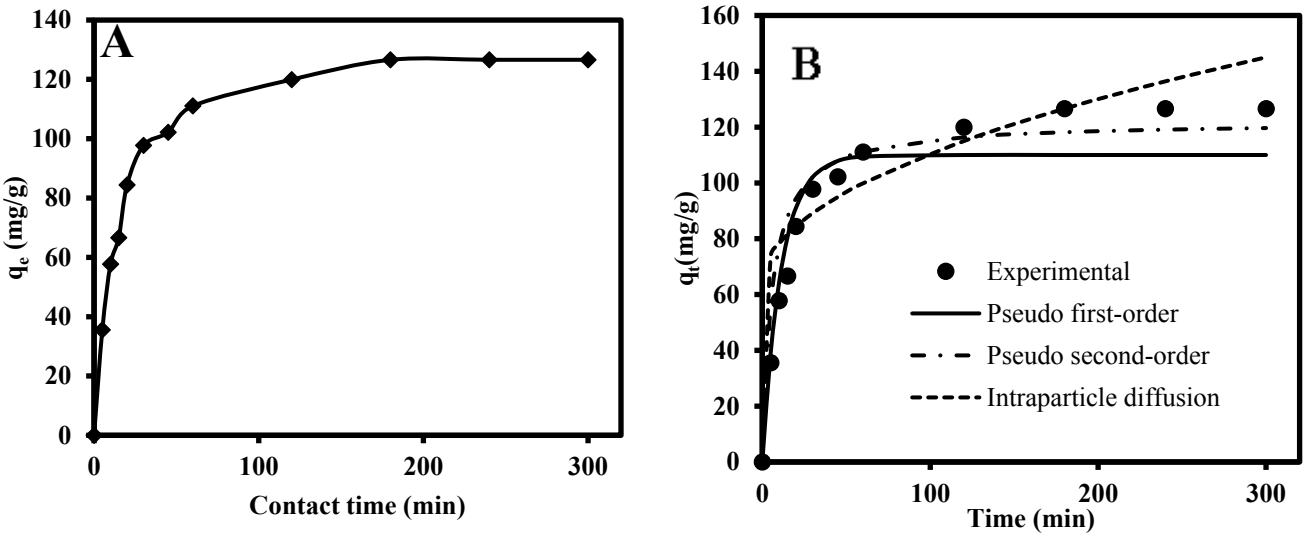


**Figure 6:** A plot of (a) the effect of contact time on Cd (II) uptake (b) adsorption kinetic plot

## 4. Conclusions

In the present work, activated charcoal (AC) was used as an adsorbent for the efficient removal of aqueous cadmium ion. The adsorbent was characterized for its surface charge, morphology and chemistry. The AC exhibited surface neutrality at pH 4.1, hence an optimum pH was established at pH 5.0 (where the AC surface charge was predominantly negative and thus implies an efficient adsorbent-adsorbate electrostatic attraction). An inverse relationship was observed between the adsorbent dosage (g/L) and uptake capacity (mg $g^{-1}$) due to the loss of adsorption capacity relating to active site clogging. Meanwhile, the Langmuir model derived maximum adsorption of 682.5 mg $g^{-1}$ was recorded at pH 5.0 and equilibrium time of ~60 min. The emergence of the Langmuir model as the isotherm model of best fit implies homogenous adsorption of Cd(II) on monolayer AC sorption sites. Similarly, the adsorption system is

considered to be predominantly chemisorption since the kinetic data were best fitted to the pseudo-second-order model. The combination of high adsorption capacity and fast equilibrium suggests that this material is a noteworthy candidate for efficient wastewater treatment.

## Conflict of interest statement

The authors declare that they have no conflict of interest.

## Data availability statement

Our manuscript has no associated data.

## References


1. Ali, H., E. Khan, and I. Ilahi, *Environmental chemistry and ecotoxicology of hazardous heavy metals: environmental persistence, toxicity, and bioaccumulation.* Journal of chemistry, 2019. **2019**.
2. Hashem, A., H.A. Hammad, and A. Al-Anwar, *Chemically modified Retama raetam biomass as a new adsorbent for Pb (II) ions from aqueous solution: non-linear regression, kinetics and thermodynamics.* Green Processing and Synthesis, 2015. **4**(6): p. 463-478.
3. Usman, A., A. Sallam, M. Zhang, M. Vithanage, M. Ahmad, A. Al-Farraj, Y.S. Ok, A. Abduljabbar, and M. Al-Wabel, *Sorption process of date palm biochar for aqueous Cd (II) removal: Efficiency and mechanisms.* Water, Air, & Soil Pollution, 2016. **227**(12): p. 1-16.
4. Masindi, V. and K.L. Muedi, *Environmental contamination by heavy metals.* Heavy metals, 2018. **10**: p. 115-132.
5. Meseguer, V.F., J.F. Ortuño, M.I. Aguilar, M.L. Pinzón-Bedoya, M. Lloréns, J. Sáez, and A.B. Pérez-Marín, *Biosorption of cadmium (II) from aqueous solutions by natural and modified non-living leaves of Posidonia oceanica.* Environmental Science and Pollution Research, 2016. **23**(23): p. 24032-24046.
6. Roe, F., *International Agency for Research on Cancer (IARC) 1976 Annual Report.* Journal of Clinical Pathology, 1978. **31**(2): p. 200.

7. Hashem, A., E. Abdel-Halim, K.F. El-Tahlawy, and A. Hebeish, *Enhancement of the adsorption of Co (II) and Ni (II) ions onto peanut hulls through esterification using citric acid.* Adsorption Science & Technology, 2005. **23**(5): p. 367-380.
8. Aniagor, C.O., C.A. Igwegbe, J.O. Ighalo, and S.N. Oba, *Adsorption of doxycycline from aqueous media: A review.* Journal of Molecular Liquids, 2021. https://doi.org/10.1016/j.molliq.2021.116124: p. 116124.
9. Boparai, H.K., M. Joseph, and D.M. O'Carroll, *Kinetics and thermodynamics of cadmium ion removal by adsorption onto nano zerovalent iron particles.* Journal of hazardous materials, 2011. **186**(1): p. 458-465.
10. Tan, G. and D. Xiao, *Adsorption of cadmium ion from aqueous solution by ground wheat stems.* Journal of hazardous materials, 2009. **164**(2-3): p. 1359-1363.
11. Pal, P. and A. Pal, *Surfactant-modified chitosan beads for cadmium ion adsorption.* International journal of biological macromolecules, 2017. **104**: p. 1548-1555.
12. Hua, Y., X. Zheng, L. Xue, L. Han, S. He, T. Mishra, Y. Feng, L. Yang, and B. Xing, *Microbial aging of hydrochar as a way to increase cadmium ion adsorption capacity: Process and mechanism.* Bioresource technology, 2020. **300**: p. 122708.
13. Yusuff, A.S., L.T. Popoola, and E.O. Babatunde, *Adsorption of cadmium ion from aqueous solutions by copper-based metal organic framework: equilibrium modeling and kinetic studies.* Applied Water Science, 2019. **9**(4): p. 1-11.
14. Hashem, A., S. Badawy, S. Farag, L. Mohamed, A. Fletcher, and G. Taha, *Non-linear adsorption characteristics of modified pine wood sawdust optimised for adsorption of Cd (II) from aqueous systems.* Journal of Environmental Chemical Engineering, 2020: p. 103966.
15. Hashem, A., M. Nasr, A. Fletcher, and L.A. Mohamed, *Aminated acrylic fabric waste derived sorbent for Cd (II) ion removal from aqueous solutions: mechanism, equilibria and kinetics.* Journal of Polymers and the Environment, 2020: p. 1-12.
16. Abdel-Halim, E., H.H. Alanazi, and S.S. Al-Deyab, *Utilization of olive tree branch cellulose in synthesis of hydroxypropyl carboxymethyl cellulose.* Carbohydrate polymers, 2015. **127**: p. 124-134.

17. Hashem, A., H. Sokker, E.A. Halim, and A. Gamal, *γ-induced graft copolymerization onto cellulosic fabric waste for cationic dye removal.* Adsorption Science & Technology, 2005. **23**(6): p. 455-466.
18. Abdel-Halim, E.S. and A.A. Al-Hoqbani, *Utilization of poly (acrylic acid)/cellulose graft copolymer for dye and heavy metal removal.* BioResources, 2015. **10**(2): p. 3112-3130.
19. Abdel-Halim, E., *Physiochemical properties of differently pretreated cellulosic fibers.* Carbohydrate polymers, 2012. **88**(4): p. 1201-1207.
20. Abdel-Halim, E.S., S.S. Al-Deyab, and A.Y.A. Alfaifi, *Cotton fabric finished with β-cyclodextrin: Inclusion ability toward antimicrobial agent.* Carbohydrate Polymers, 2014. **102**(1): p. 550-556.
21. ANIAGOR, C.O. and M.C. MENKITI, *RELATIONAL DESCRIPTION OF AN ADSORPTION SYSTEM BASED ON ISOTHERM, ADSORPTION DENSITY, ADSORPTION POTENTIAL, HOPPING NUMBER AND SURFACE COVERAGE.* Sigma, 2020. **38**(3): p. 1073-1098.
22. Hegyesi, N., R.T. Vad, and B. Pukánszky, *Determination of the specific surface area of layered silicates by methylene blue adsorption: The role of structure, pH and layer charge.* Applied Clay Science, 2017. **146**: p. 50-55.
23. Jia, Y. and K. Thomas, *Adsorption of cadmium ions on oxygen surface sites in activated carbon.* Langmuir, 2000. **16**(3): p. 1114-1122.
24. Uğurlu, M., A. Gürses, and M. Açıkyıldız, *Comparison of textile dyeing effluent adsorption on commercial activated carbon and activated carbon prepared from olive stone by ZnCl2 activation.* Microporous and Mesoporous Materials, 2008. **111**(1-3): p. 228-235.
25. Osasona, I., K. Aiyedatiwa, J. Johnson, and O.L. Faboya, *Activated carbon from spent brewery barley husks for cadmium ion adsorption from aqueous solution.* Indonesian Journal of Chemistry, 2018. **18**(1): p. 145-152.
26. Nejadshafiee, V. and M.R. Islami, *Adsorption capacity of heavy metal ions using sultone-modified magnetic activated carbon as a bio-adsorbent.* Materials Science and Engineering: C, 2019. **101**: p. 42-52.

27. Alkherraz, A.M., A.K. Ali, and K.M. Elsherif, *Removal of Pb (II), Zn (II), Cu (II) and Cd (II) from aqueous solutions by adsorption onto olive branches activated carbon: equilibrium and thermodynamic studies.* Chemistry International, 2020. **6**(1): p. 11-20.
28. Manjuladevi, M., R. Anitha, and S. Manonmani, *Kinetic study on adsorption of Cr (VI), Ni (II), Cd (II) and Pb (II) ions from aqueous solutions using activated carbon prepared from Cucumis melo peel.* Applied water science, 2018. **8**(1): p. 1-8.
29. Sharma, G. and M. Naushad, *Adsorptive removal of noxious cadmium ions from aqueous medium using activated carbon/zirconium oxide composite: isotherm and kinetic modelling.* Journal of Molecular Liquids, 2020. **310**: p. 113025.
30. Xie, X., H. Gao, X. Luo, T. Su, Y. Zhang, and Z. Qin, *Polyethyleneimine modified activated carbon for adsorption of Cd (II) in aqueous solution.* Journal of Environmental Chemical Engineering, 2019. **7**(3): p. 103183.
31. Zhang, Z., T. Wang, H. Zhang, Y. Liu, and B. Xing, *Adsorption of Pb (II) and Cd (II) by magnetic activated carbon and its mechanism.* Science of The Total Environment, 2021. **757**: p. 143910.
32. Ioannidou, O. and A. Zabaniotou, *Agricultural residues as precursors for activated carbon production—a review.* Renewable and sustainable energy reviews, 2007. **11**(9): p. 1966-2005.
33. Langmuir, I., *The constitution and fundamental properties of solids and liquids. Part I. Solids.* Journal of the American chemical society, 1916. **38**(11): p. 2221-2295.
34. Igwegbe, C.A., S.N. Oba, C.O. Aniagor, A.G. Adeniyi, and J.O. Ighalo, *Adsorption of ciprofloxacin from water: a comprehensive review.* Journal of Industrial and Engineering Chemistry, 2020.
35. Igwegbe, C.A., O.D. Onukwuli, J.O. Ighalo, and P.U. Okoye, *Adsorption of cationic dyes on Dacryodes edulis seeds activated carbon modified using phosphoric acid and sodium chloride.* Environmental Processes, 2020. **7**(4): p. 1151-1171.
36. Wohleber, D.A. and M. Manes, *Application of the Polanyi adsorption potential theory to adsorption from solution on activated carbon. III. Adsorption of miscible organic liquids from water solution.* The Journal of Physical Chemistry, 1971. **75**(24): p. 3720-3723.
37. Freundlich, H., *Über die adsorption in lösungen.* Zeitschrift für physikalische Chemie, 1907. **57**(1): p. 385-470.

38. Temkin, M., *Kinetics of ammonia synthesis on promoted iron catalysts.* Acta physiochim. URSS, 1940. **12**: p. 327-356.
39. Aniagor, C. and M. Menkiti, *Kinetics and mechanistic description of adsorptive uptake of crystal violet dye by lignified elephant grass complexed isolate.* Journal of Environmental Chemical Engineering, 2018. **6**(2): p. 2105-2118.
40. Lagergren, S.K., *About the theory of so-called adsorption of soluble substances.* Sven. Vetenskapsakad. Handingarl, 1898. **24**: p. 1-39.
41. Ho, Y.-S. and G. McKay, *Pseudo-second order model for sorption processes.* Process biochemistry, 1999. **34**(5): p. 451-465.
42. Weber, W.J. and J.C. Morris, *Kinetics of adsorption on carbon from solution.* Journal of the sanitary engineering division, 1963. **89**(2): p. 31-60.
43. Kumar, K.V. and S. Sivanesan, *Pseudo second order kinetics and pseudo isotherms for malachite green onto activated carbon: comparison of linear and non-linear regression methods.* Journal of Hazardous Materials, 2006. **136**(3): p. 721-726.
44. Menkiti, M., M. Abonyi, and C. Aniagor, *Process Equilibrium, Kinetics, and Mechanisms of Ionic-Liquid Induced Dephenolation of Petroleum Effluent.* Water Conservation Science and Engineering, 2018. **3**(3): p. 205-220.
45. El-Khaiary, M.I. and G.F. Malash, *Common data analysis errors in batch adsorption studies.* Hydrometallurgy, 2011. **105**(3-4): p. 314-320.
46. Menkiti, M., C. Aniagor, C. Agu, and V. Ugonabo, *Effective adsorption of crystal violet dye from an aqueous solution using lignin-rich isolate from elephant grass.* Water Conservation Science and Engineering, 2018. **3**(1): p. 33-46.
47. Nandiyanto, A.B.D., R. Oktiani, and R. Ragadhita, *How to read and interpret FTIR spectroscope of organic material.* Indonesian Journal of Science and Technology, 2019. **4**(1): p. 97-118.
48. Conley, R.T. and J.F. Bieron, *Examination of the oxidative degradation of polyacrylonitrile using infrared spectroscopy.* Journal of Applied Polymer Science, 1963. **7**(5): p. 1757-1773.
49. Ngah, W.W., L. Teong, R. Toh, and M. Hanafiah, *Utilization of chitosan–zeolite composite in the removal of Cu (II) from aqueous solution: adsorption, desorption and fixed bed column studies.* Chemical Engineering Journal, 2012. **209**: p. 46-53.

50. Nwosu, F.O., O.J. Ajala, R.M. Owoyemi, and B.G. Raheem, *Preparation and characterization of adsorbents derived from bentonite and kaolin clays.* Applied Water Science, 2018. **8**(7): p. 1-10.
51. Hashem, A., C. Aniagor, G. Taha, and M. Fikry, *Utilization of Low-cost Sugarcane Waste for the Adsorption of Aqueous Pb(II): Kinetics and Isotherm Studies.* Current Research in Green and Sustainable Chemistry, 2021. 10.1016/j.crgsc.2021.100056.
52. Hashem, A., A. Abou-Okeil, M. Fikry, A. Aly, and C.O. Aniagor, *Isotherm and Kinetics Parametric Studies for Aqueous Hg(II) Uptake onto N-[2-(Methylamino)Ethyl]Ethane-1,2-Diaminated Acrylic Fibre.* Arabian Journal for Science and Engineering, 2021. https://doi.org/10.1007/s13369-021-05416-x.
53. Hamdaoui, O., *Batch study of liquid-phase adsorption of methylene blue using cedar sawdust and crushed brick.* Journal of hazardous materials, 2006. **135**(1-3): p. 264-273.
54. Hashem, A., C.O. ANIAGOR, M. Nasr, and A. Abou-Okeil, *Efficacy of treated sodium alginate and activated carbon fibre for Pb(II) adsorption.* International journal of biological macromolecules, 2021. https://doi.org/10.1016/j.ijbiomac.2021.02.067: p. 1-16.
55. Chen, H., Y. Zhao, and A. Wang, *Removal of Cu (II) from aqueous solution by adsorption onto acid-activated palygorskite.* Journal of Hazardous Materials, 2007. **149**(2): p. 346-354.
56. Aniagor, C., E. Abdel-Halim, and A. Hashem, *Evaluation of the Aqueous Fe (II) ion Sorption Capacity of Functionalized Microcrystalline Cellulose.* Journal of Environmental Chemical Engineering, 2021. https://doi.org/10.1016/j.jece.2021.105703: p. 105703.
57. Alhan, S., M. Nehra, N. Dilbaghi, N.K. Singhal, K.-H. Kim, and S. Kumar, *Potential use of ZnO@ activated carbon nanocomposites for the adsorptive removal of Cd2+ ions in aqueous solutions.* Environmental research, 2019. **173**: p. 411-418.
58. Kannan, N. and M.M. Sundaram, *Kinetics and mechanism of removal of methylene blue by adsorption on various carbons—a comparative study.* Dyes and pigments, 2001. **51**(1): p. 25-40.